Archive of Applied Mechanics (2023) 93:2191–2207
https://doi.org/10.1007/s00419-023-02379-3

ORIGINAL

M. Javed Idrisi · M. Shahbaz Ullah · Getachew Mulu · Worku Tenna · Andualem Derebe

The circular restricted eight-body problem

Received: 23 August 2022 / Accepted: 8 February 2023 / Published online: 2 March 2023

Abstract We study the motion of infinitesimal mass in the vicinity of the dominant primaries under the Newtonian law of gravitation in the restricted eight-body problem. The proposed problem is a particular case of $n + 1$-body problem studied by Kalvouridis (Astrophys. Space Sci 260: 309 325, 1999). We consider six peripheral primaries $P_1, P_2, \ldots, P_6$, each of mass m, revolve in a circular orbit of radius a with an angular velocity ω about their common center of mass. The primaries P_i $(i = 1, 2, \ldots, 6)$ are revolve in a way such that P_1, P_3, P_5 and P_2, P_4, P_6 always form equilateral triangles of side l and have a common circumcenter where the seventh more massive primary P_0 of mass m_0 rests. The primaries form a symmetric configuration with respect to the origin at any instant of time. This is observed that there exist 18 equilibrium points out of which four equilibrium points are on x-axis, two on y-axis and rest are in orbital plane of the primaries. All the equilibrium points lie on the concentric circles C_1, C_2 andC_3 centered at origin and there exists exactly six equilibrium points on each circle. The equilibrium points on circle C_2 are stable for the critical mass parameter β_0 while the equilibrium points on circles C_1 and C_3 are unstable for all values of mass parameter β. The regions of motion for infinitesimal mass are also analyzed in this paper.

Keywords Restricted n-body problem · Equilibrium points · Linear stability · Regions of motion

1 Introduction

In the last decades many authors have put their efforts in solving the restricted problem of more than three-bodies in different aspects. Their work is appreciable and encouraged us to develop a configuration in restricted problem of eight bodies' to describe the motion of spacecraft in the vicinity of the dominant primaries.

The restricted three-body problem plays an important role to understand the behavior of satellite in the vicinity of two dominant primaries. This model is suitable to understand the dynamics of satellite in Earth-

M. J. Idrisi (✉) · W. Tenna · A. Derebe
Department of Mathematics, College of Natural and Computational Science, Mizan-Tepi University, Tepi, Ethiopia
e-mail: javed@mtu.edu.et

W. Tenna
e-mail: workuworku12@gmail.com

A. Derebe
e-mail: andualemderebe388@gmail.com

M. S. Ullah
Department of Mathematics, Zakir Husain Delhi College, New Delhi 110002, India
e-mail: mdshahbazbgp@gmail.com

G. Mulu
Department of Physics, College of Natural and Computational Science, Mizan-Tepi University, Tepi, Ethiopia
e-mail: getachew2721@gmail.com

Moon and Sun-Earth planet system. A lot of research papers have been written in last five decades to show the significance of the equilibrium points obtained in these systems by including many parameters as oblateness of the primaries, radiation pressure, PR-drag effect, albedo effect etc. The stability of the triangular points in the elliptic restricted problem of three bodies is studied by Danby [12]. A concise solution to the restricted three-body problem in the circular as well as in the elliptical case has been found by Szebehely [41]. The restricted three-body problem under the consideration of radiation pressure has been studied by Chernikov [8]. The equilibrium points in the generalized elliptic restricted three-body problem are investigated by Choudhary [9]. Bhatnagar and Hallan [4] have studied the effect of perturbed potentials on the stability of equilibrium points in the restricted problem of three bodies. Asymptotic solutions to the restricted problem near equilateral equilibrium points have been investigated by Cid et al. [10]. Markellos et al. [31] have discussed the nonlinear stability zones around triangular equilibria in the plane circular restricted three-body problem with oblateness. Roberts [37] has examined the linear stability of the triangular equilibrium points in the elliptic restricted three-body problem. Douskos [14] has analyzed the collinear equilibrium points of Hill's problem with radiation and oblateness and their fractal basins of attraction. Idrisi and Taqvi [18, 19] have solved the circular restricted three-body problem in terms of elliptic integrals. The restricted three-body problem under the consideration of albedo effects in circular and elliptic cases is studied by Idrisi [20], Idrisi and Ullah [21–23, 25, 43]. Ershkov and Leshchenko [15] have presented an approach for solving the Euler-Poisson equations of momentum near the liberation points for planets in our Solar System whose orbital plane is inclined relative to Earth's orbit. In a recent study conducted by Ershkov et al. [16], a semi-analytical approach was employed to analyze the bi-elliptic problem of four bodies and explore possible stable positioning for elements of a Dyson sphere.

The following researchers have extended the restricted three-body problem to 4-body, 5-body, 6-body and in general n-body problem: Michalodimitrakis [32] has investigated the equilibrium points, zero velocity curves and periodic orbits around the equilibrium points in the restricted four-body problem. Pacella [33] has used the equivariant Morse theory in three-dimensional n-body problem to estimate the minimal number of central configurations. In this study it is shown that the non-planar central configurations exist for $n \geq 4$. Casasayas et al. [5] have considered a restricted charged four-body problem and proved the existence of infinite symmetric periodic orbits with arbitrarily large extremal period. The global solution of the n-body problem using a new 'blowing up' transformation is given by Qiu-Dong [36]. Roy et al. [38] have investigated some special cases of restricted four-body problems. Kalvouridis [27] has studied $n + 1$-body problem by arranging the peripheral primaries in equal arcs on an ideal ring with a central body of different mass is considered at the center of mass of the system. Bang et al. [3] have proved results on the existence and on linear stability of equilibrium points in the restricted $N + 1$ body problem. Celli [6] has studied the central configurations of four masses in detail. Baltagiannis et al. [2] have studied the existence of equilibrium points and their linear stability in the equilateral configuration of restricted four-body problem. A study of finding central configurations of the four-body problem with a dominant mass was carried out by Corbera et al. [11]. Kumari et al. [28] have plotted the equilibrium points and zero velocity surfaces in the restricted four-body problem with solar wind drag. Papadouris et al. [34] have examined the existence of equilibrium points and their linear stability in the equilateral configuration of restricted four-body problem with radiation pressure. A new perturbative method for solving the gravitational n-body problem in the general theory of relativity is given by Turyshev and Toth [42]. Marchesin [30] has considered a rhomboidal configuration of restricted five-body problem and discussed the stability of rhomboidal equilibria. Gao et al. [17] have analyzed the equilibrium points and zero velocity surfaces in the axisymmetric central configuration of restricted five-body problem. A special case of the restricted four-body problem has been investigated by Ansari [1] by treating the three primaries as a triaxial rigid body and the infinitesimal body as variable mass. An inverse problem of central configurations in the collinear five-body problem has been investigated by Davis et al. [13]. Ullah et al. [43] have studied the elliptic Sitnikov five-body problem under the consideration of radiation pressure. Idrisi and Ullah [23] have studied the existence and stability of equilibrium points in restricted six-body problem under a square configuration model. Chen and Yang [7] have examined the central configurations of five-body problem with four infinitesimal particles out of which two particles have unequal mass. Pappalarado et al. [35] have used an analytical approach based on the direct linearization of the index-three form to analyze the stability of multibody mechanical systems in the framework of Lagrangian mechanics. Ullah et al. [44] have probed the Sitnikov five-body problem with combined effects of radiation pressure and oblateness. Idrisi et al. [24] have shown the effect of perturbations in Coriolis and centrifugal forces on equilibrium points in the restricted six-body problem. The stability analysis of rhomboidal restricted six-body problem is studied by Siddique et al. [39]. The motion of infinitesimal mass around out-of-plane equilibrium points in the frame of restricted six-body problem under radiation pressure is examined by Idrisi and Ullah [26]. Siddique and Kashif [40] have

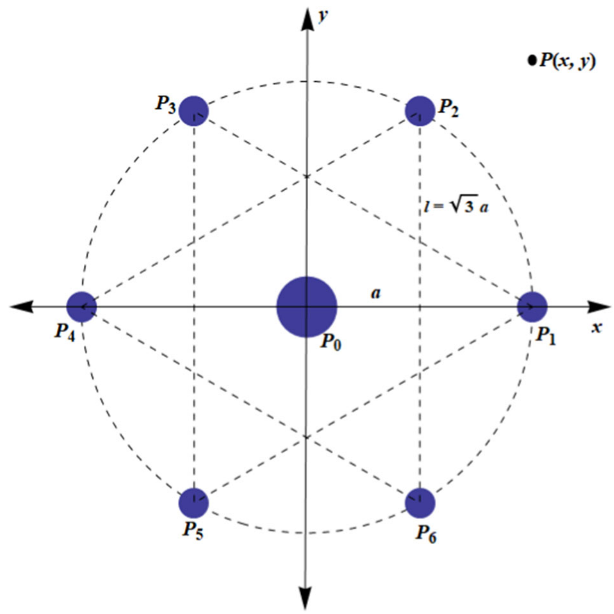

Fig. 1 Configuration of restricted eight-body problem

explored the stable equilibrium points in the rhomboidal restricted six-body problem. The periodic solutions of circular Sitnikov restricted four-body problem using multiple scales method are analyzed by Kumari et al. [29].

In this paper, we have considered a symmetric configuration of restricted eight-body problem in which the dominant primary is located at the center of mass of the system. The paper is organized as follows: In Sect. 1, some notable researches related to the theme of the research are given. The mathematical model of the system and equations of motion of infinitesimal mass are obtained in Sect. 2. The graphical and numerical solution to equilibrium points are given in Sect. 3. In Sect. 4, the stability of equilibrium points is discussed. The regions of motion or zero velocity regions are discussed in brief in Sect. 5. In the last section, conclusions are drawn.

2 Mathematical model and equations of motion

Let six peripheral primaries P_1, P_2, …, P_6, each of mass m, revolve in a circular orbit of radius a with an angular velocity ω about their common center of mass O. The primaries P_i $(i = 1, 2, \ldots, 6)$ are revolve in a way such that P_1, P_3, P_5 and P_2, P_4, P_6 always form equilateral triangles of side l and have a common circumcenter where the seventh more massive primary P_0 of mass m_0 rests (Fig. 1). It is also assumed that the mass of central primary is greater than the sum of all masses of peripheral primaries, i.e., $m_0 > \Sigma m_i$, $i = 1, 2, \ldots, 6$. The orbit lies in the Oxy plane of the inertial frame of reference, and has its center at the origin. According to Newton's law of gravitation, primaries attract each other and at any instant of time form a symmetric configuration with respect to the origin. Suppose that a test particle P with infinitesimal mass $m' << 1$ moves under the gravitational field of P_i $(i = 0, 1, \ldots, 6)$ in the same plane. The distances of P from O and P_i $(i = 1, 2, \ldots, 6)$ are $\boldsymbol{r_0}$ and $\boldsymbol{r_i}$ $(i = 1, 2, \ldots, 6)$**,** respectively. From Fig. 1, it can be seen that the proposed configuration is possible if $l = \sqrt{3}a$ where l and a are the dimensionless lengths of side of equilateral triangles and radius of circular orbit, respectively.

In order to maintain the configuration of the primaries, the sum of the gravitational forces applied by P_0, P_2, P_3, P_4, P_5 and P_6 on P_1 must be equal to the centrifugal force, *i.e.,*

$$m_1\, \vec{OP_1}\, \omega^2 = \frac{Gm_0 m_1\, \vec{OP_1}}{|OP_1|^3} + \sum_{j=2}^{6} \frac{Gm_j m_1\, \vec{P_j P_1}}{|P_j P_1|^3},$$

which gives

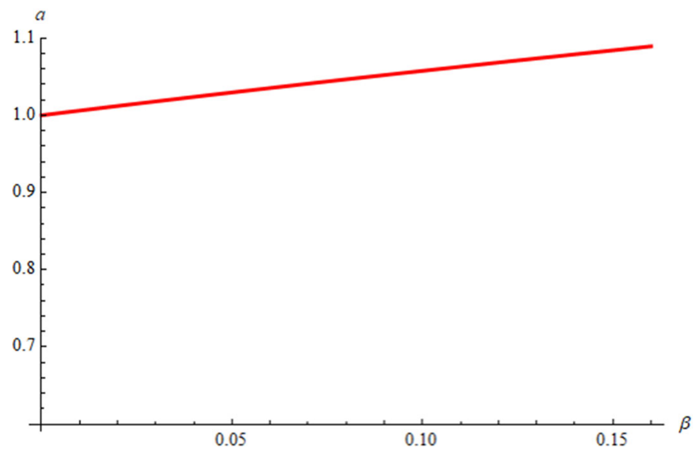

Fig. 2 a with respect to β

$$\omega^2 = \frac{Gm_0}{a^3}\left(1 + \kappa\frac{m}{m_0}\right),\ \kappa = 1.82735.$$

Now, we choose the units of distance, mass and time in such a way that $G = 1$, $m_0 = 1$ and $\omega = 1$, therefore we have $a = (1 + k\ \beta)^{1/3}$, $\beta = m/m_0$ is the mass parameter having the range $0 < \beta < 1/6$. Obviously, a is an increasing function in terms of β and thus as mass parameter β increases the radius of the orbit of primaries also increases (Fig. 2).

2.1 Equations of motion

The equations of motion of the particle $P(x, y, z)$ in the synodic coordinate system and dimensionless variables are given by

$$\ddot{x} - 2\dot{y} = \frac{\partial U}{\partial x},\quad \ddot{y} + 2\dot{x} = \frac{\partial U}{\partial y} \text{ and } \ddot{z} = \frac{\partial U}{\partial z} \tag{1}$$

where the effective potential U may be written as

$$\begin{aligned}
U &= \frac{1}{2}(x^2 + y^2) + \frac{1}{r_0} + \sum_{\upsilon=1}^{6}\frac{\beta}{r_\upsilon},\\
r_0^2 &= x^2 + y^2 + z^2,\\
r_\upsilon^2 &= (x - x_\upsilon)^2 + (y - y_\upsilon)^2 + z^2,\\
x_\upsilon &= a\cos\left[(\upsilon - 1)\frac{\pi}{3}\right],\ y_\upsilon = a\sin\left[(\upsilon - 1)\frac{\pi}{3}\right], \upsilon = 1,\ 2,\ \ldots,\ 6.
\end{aligned}$$

The integral analogous to Jacobi integral is

$$v^2 = 2U - c, \tag{2}$$

where v is the velocity of the particle P having infinitesimal mass m' and c is Jacobian constant.

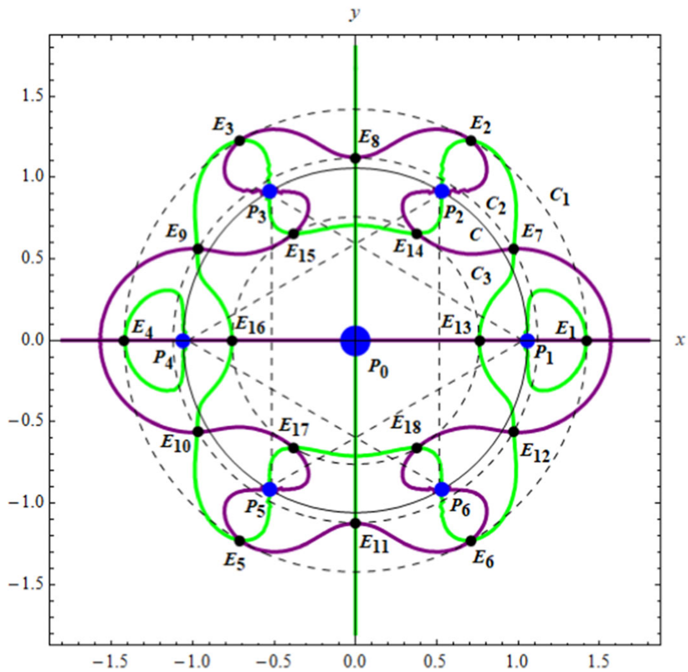

Fig. 3 Equilibrium Points E_i ($i = 1, 2, \ldots, 18$) in orbital plane for $\beta = 0.1$

3 Equilibrium points in orbital plane

The equilibrium points in orbital plane are the solution of the Eqns. $U_x = 0, U_y = 0$ and $z = 0$, i.e.,

$$\left.\begin{aligned} U_x &= \left(1 - \frac{1}{r_0^3}\right)x - \beta \sum_{\upsilon=1}^{6} \frac{(x - x_\upsilon)}{r_\upsilon^3} = 0, \\ U_y &= \left(1 - \frac{1}{r_0^3}\right)y - \beta \sum_{\upsilon=1}^{6} \frac{(y - y_\upsilon)}{r_\upsilon^3} = 0. \end{aligned}\right\} \tag{3}$$

3.1 Graphical solution to equilibrium points

Clearly, the equilibrium points are the intersection of the curves $U_x(x, y)$ and $U_y(x, y)$. On plotting the corresponding curves it turns out that there are 18 equilibrium points, four of which are collinear and fourteen are non-collinear (Fig. 3). All points of equilibrium lie on the concentric circles C_1, C_2 andC_3 centered at the origin. The equilibrium points E_i ($i = 1, 2, \ldots, 6$) lie on circle C_1, E_j ($j = 7, 8, \ldots, 12$) on C_2 and E_k ($k = 13, 14, \ldots, 18$) on C_3. Further, it is observed that the six equilibrium points are on the axes and twelve are in orbital plane of the primaries, i.e., E_1, E_4, E_{13} and E_{16} are on *x-axis*, E_8 and E_{11} on *y-axis* and rest are in the orbital plane.

3.2 Numerical solution

In this section, we locate the equilibrium points numerically on the circles C_1, C_2 and C_3 using Newton–Raphson iteration method. Instead of finding all the equilibrium points, we focus on just one equilibrium point on each circle C_1, C_2 and C_3, i.e., E_1, E_8 and E_{13} and the locations of other equilibrium points can be found by symmetricity. Let us assume that the coordinates of E_1, E_8 and E_{13} be $(a + \rho, 0)$, $(0, a + \lambda)$ and $(a–\delta, 0)$, respectively (Fig. 4), where $\rho, \lambda, \delta \in \boldsymbol{R}^{+}$.

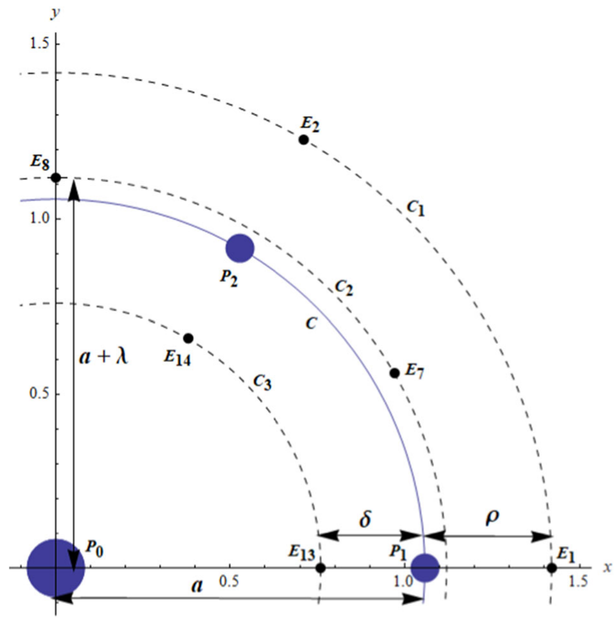

Fig. 4 Locations of E_1, E_8 and E_{13}

3.2.1 Equilibrium points on $\boldsymbol{C}_1$

First we find the location of equilibrium point E_1 and then by symmetricity we can locate other equilibrium points on C_1. Let the coordinates of E_1 be $(a+\rho, 0)$. Thus, on substituting $x = a + \rho$ and $y = 0$ in Eq. (3), we have $f(\rho) = 0$, where

$$\begin{aligned} f(\rho) &= f_1(\rho) - \beta f_2(\rho) = 0, \\ f_1(\rho) &= (a+\rho)\left(1 - \frac{1}{(a+\rho)^3}\right), \\ f_2(\rho) &= \frac{1}{\rho^2} + \frac{1}{(2a+\rho)^2} + \frac{a+2\rho}{(a^2+a\rho+\rho^2)^{3/2}} + \frac{3a+2\rho}{(3a^2+3a\rho+\rho^2)^{3/2}}. \end{aligned} \tag{4}$$

The solution of Eq. (4) provides the location of E_1. Since the general solution of Eq. (4) is not possible therefore we apply Newton–Raphson iteration method to solve it. On solving Eq. (4) for various values of mass parameter β, we have only one positive real root as shown in Fig. 5. It is observed that as the mass parameter β increases, ρ increases and the equilibrium point E_1 moves away from the primary P_1 along x-axis. The numerical positions of E_1 and other equilibrium points on C_1 for various values of mass parameter β are given in Table 1. The coordinates of the equilibrium points $E_i(x_i, y_i)$ lying on C_1 are given by:

$$x_i = \Lambda \cos\left((i-1)\frac{\pi}{3}\right),\ y_i = \Lambda \sin\left((i-1)\frac{\pi}{3}\right),\ i = 1, 2, \ldots, 6$$

where $\Lambda = a + \rho$ is the radius of circle C_1.

3.2.2 Equilibrium points on $\boldsymbol{C}_2$

Let the coordinates of E_8 be $(0, a+\lambda)$. Thus on substituting $x = 0$ and $y = a + \lambda$ in Eq. (3), we have $g(\lambda) = 0$, where

$$g(\lambda) = g_1(\lambda) - \beta g_2(\lambda) = 0, \tag{5}$$

$$g_1(\lambda) = (a+\lambda)\left(1 - \frac{1}{(a+\lambda)^3}\right),$$

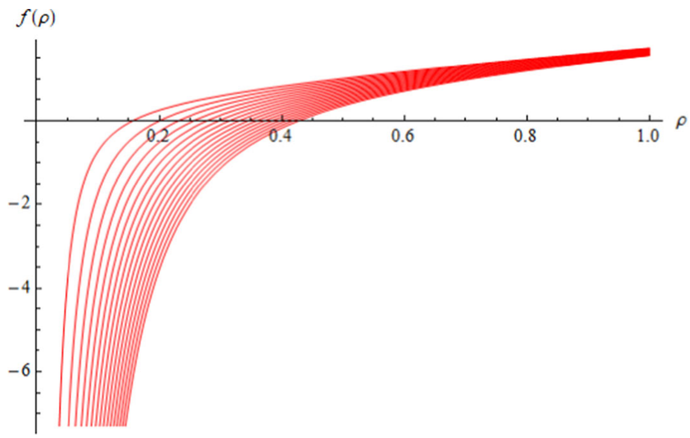

Fig. 5 Zeroes of $f(\rho)$ for different values of mass parameter β

Table 1 Equilibrium points on C_1

β	a	ρ	Λ	$E_{1,4}$	$E_{2,6}$	$E_{3,5}$
0.01	1.006054	0.156886	1.162940	(±1.162940, 0)	(0.581470, ±1.007136)	(− 0.581470, ±1.007136)
0.02	1.012037	0.200297	1.212334	(±1.212334, 0)	(0.606167, ±1.049912)	(− 0.606167, ±1.049912)
0.04	1.023794	0.256691	1.280485	(±1.280485, 0)	(0.640243, ±1.108933)	(− 0.640243, ±1.108933)
0.06	1.035287	0.297393	1.332680	(±1.332680, 0)	(0.666340, ±1.154135)	(− 0.666340, ±1.154135)
0.08	1.046531	0.330452	1.376982	(±1.376982, 0)	(0.688491, ±1.192502)	(− 0.688491, ±1.192502)
0.10	1.057538	0.358799	1.416337	(±1.416337, 0)	(0.708168, ±1.226583)	(− 0.708168, ±1.226583)
0.12	1.068320	0.383881	1.452201	(±1.452201, 0)	(0.726101, ±1.257643)	(− 0.726101, ±1.257643)
0.14	1.078889	0.406532	1.485421	(±1.485421, 0)	(0.742711, ±1.286412)	(− 0.742711, ±1.286412)
0.16	1.089255	0.427284	1.516539	(±1.516539, 0)	(0.758270, ±1.313361)	(− 0.758270, ±1.313361)

$$g_2(\lambda) = \frac{2(a+\lambda)}{(2a^2+2a\lambda+\lambda^2)^{3/2}} + \frac{(2-\sqrt{3})a+2\lambda}{((2-\sqrt{3})a^2+(2-\sqrt{3})a\lambda+\lambda^2)^{3/2}} + \frac{(2+\sqrt{3})a+2\lambda}{((2+\sqrt{3})a^2+(2+\sqrt{3})a\lambda+\lambda^2)^{3/2}}.$$

On solving Eq. (5) for different values of mass parameter β by Newton–Raphson iteration method, we have location of E_8. Eq. (5) possesses only one real root for $0<\beta<1/6$ as shown in Fig. 6. It is found that λ increases as the mass parameter β increases and the equilibrium point E_8 moves in upward direction along y-axis. The numerical positions of E_8 and other equilibrium points on C_2 for various values of mass parameter β are given in Table 2. The coordinates of the equilibrium points $E_j(x_j, y_j)$ lying on C_2 are given by:

$$x_j = \tau\cos\Big((2j-13)\frac{\pi}{6}\Big),\ y_j = \tau\sin\Big((2j-13)\frac{\pi}{6}\Big),\ \ j=7,\ 8,\ \ldots,\ 12$$

where $\tau = a+\lambda$ is the radius of circle C_2.

3.2.3 Equilibrium points on C_3

Let the coordinates of E_{13} be $(a-\delta, 0)$. Thus on substituting $x=a-\delta$ and $y=0$ in Eq. (3), we have $h(\delta)=0$, where

$$h(\delta) = h_1(\delta) - \beta\, h_2(\delta) = 0, \tag{6}$$

$$h_1(\delta) = (a-\delta)\Big(1-\frac{1}{(a-\delta)^3}\Big),$$

$$h_2(\delta) = \frac{1}{\delta^2} + \frac{1}{(2a-\delta)^2} + \frac{a-2\delta}{(a^2-a\delta+\delta^2)^{3/2}} + \frac{3a-2\delta}{(3a^2-3a\delta+\delta^2)^{3/2}}.$$

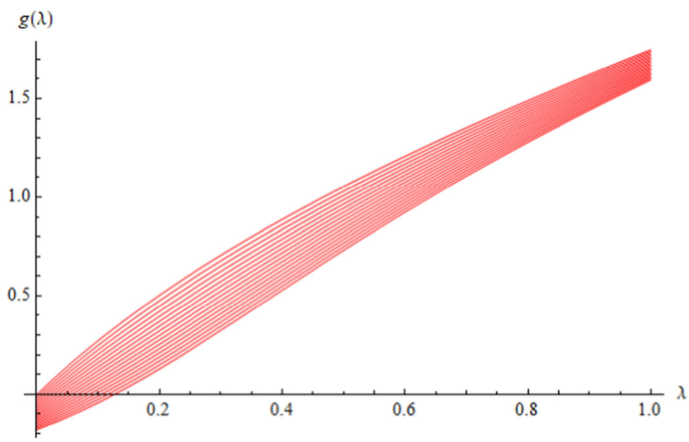

Fig. 6 Zeroes of $g(\lambda)$ for different values of mass parameter β

Table 2 Equilibrium points on C_2

B	a	Λ	τ	$E_{7,12}$	$E_{8,11}$	$E_{9,10}$
0.01	1.006054	0.004612	1.010666	$(0.875263, \pm 0.505333)$	$(0, \pm 1.010666)$	$(-0.875263, \pm 0.505333)$
0.02	1.012037	0.009607	1.021644	$(0.884770, \pm 0.510822)$	$(0, \pm 1.021644)$	$(-0.884770, \pm 0.510822)$
0.04	1.023794	0.020851	1.044645	$(0.904689, \pm 0.522323)$	$(0, \pm 1.044645)$	$(-0.904689, \pm 0.522323)$
0.06	1.035287	0.033932	1.069219	$(0.925971, \pm 0.534611)$	$(0, \pm 1.069219)$	$(-0.925971, \pm 0.534611)$
0.08	1.046531	0.048981	1.095512	$(0.948741, \pm 0.547756)$	$(0, \pm 1.095512)$	$(-0.948741, \pm 0.547756)$
0.10	1.057538	0.065993	1.123531	$(0.973006, \pm 0.561765)$	$(0, \pm 1.123531)$	$(-0.973006, \pm 0.561765)$
0.12	1.068320	0.084764	1.153084	$(0.998600, \pm 0.576542)$	$(0, \pm 1.153084)$	$(-0.998600, \pm 0.576542)$
0.14	1.078889	0.104884	1.183773	$(1.025178, \pm 0.591887)$	$(0, \pm 1.183773)$	$(-1.025178, \pm 0.591887)$
0.16	1.089255	0.125815	1.215070	$(1.052282, \pm 0.607535)$	$(0, \pm 1.215070)$	$(-1.052282, \pm 0.607535)$

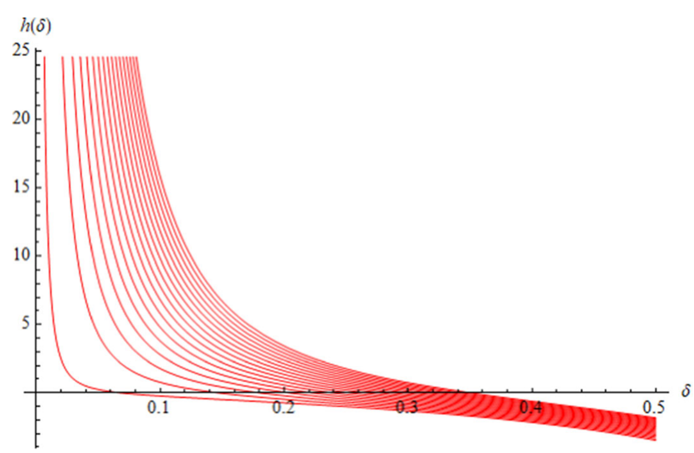

Fig. 7 Zeroes of $h(\delta)$ for different values of mass parameter β

On solving Eq. (6) for various values of mass parameter β by Newton–Raphson iteration method, we have location of E_{13}. Eq. (6) possesses only one real root for $0<\beta<1/6$ as shown in Fig. 7. It is observed that as the mass parameter β increases, δ decreases and the equilibrium point E_{13} moves toward the primary P_1 along x-axis. The numerical positions of E_{13} and other equilibrium points on C_3 for various values of mass parameter β are given in Table 3. The coordinates of the equilibrium points $E_k(x_k, y_k)$ on C_3 are given by:

$$x_k = \varepsilon \cos\left((k-13)\frac{\pi}{3}\right), \; y_k = \varepsilon \sin\left((k-13)\frac{\pi}{3}\right), \; k = 13, \; 14, \; \ldots, \; 18$$

where $\varepsilon = a - \delta$ is the radius of circle C_3.

Finally, it is concluded that there exist 18 equilibrium points $(E_1, E_2, \ldots, E_{18})$ in total and in particular 6 equilibrium points on each circle C_1, C_2 and C_3, respectively. The equilibrium points $E_1, E_2, \ldots, E_6$ are lying

Table 3 Equilibrium points on C_3

B	a	δ	E	$E_{13,16}$	$E_{14,18}$	$E_{15,17}$
0.01	1.006054	0.142242	0.863812	$(\pm 0.863812, 0)$	$(0.431906, \pm 0.748083)$	$(-0.431906, \pm 0.748083)$
0.02	1.012037	0.177374	0.834663	$(\pm 0.834663, 0)$	$(0.417331, \pm 0.722839)$	$(-0.417331, \pm 0.722839)$
0.04	1.023794	0.221256	0.802538	$(\pm 0.802538, 0)$	$(0.401269, \pm 0.695018)$	$(-0.401269, \pm 0.695018)$
0.06	1.035287	0.25212	0.783167	$(\pm 0.783167, 0)$	$(0.391584, \pm 0.678243)$	$(-0.391584, \pm 0.678243)$
0.08	1.046531	0.276931	0.769599	$(\pm 0.769599, 0)$	$(0.384801, \pm 0.666493)$	$(-0.384801, \pm 0.666493)$
0.10	1.057538	0.298146	0.759392	$(\pm 0.759392, 0)$	$(0.379697, \pm 0.657652)$	$(-0.379697, \pm 0.657652)$
0.12	1.068320	0.316948	0.751372	$(\pm 0.751372, 0)$	$(0.375686, \pm 0.650707)$	$(-0.375686, \pm 0.650707)$
0.14	1.078889	0.334004	0.744885	$(\pm 0.744885, 0)$	$(0.372443, \pm 0.645089)$	$(-0.372443, \pm 0.645089)$
0.16	1.089255	0.349728	0.739527	$(\pm 0.739527, 0)$	$(0.369764, \pm 0.640449)$	$(-0.369764, \pm 0.640449)$

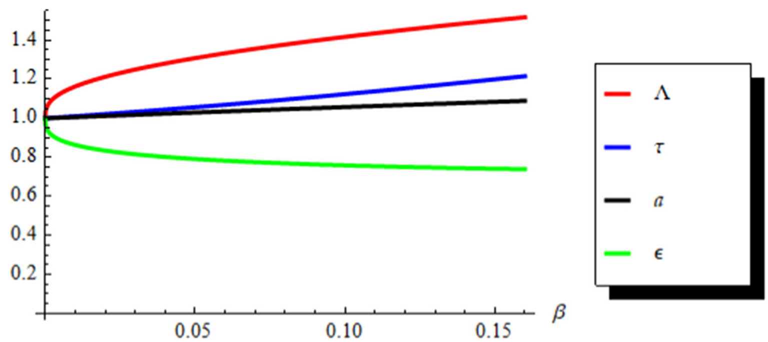

Fig. 8 Radius of C_1, C_2, C and C_3 with respect to β

on circle C_1; $E_7, E_8, \ldots, E_{12}$ on circle C_2 and $E_{13}, E_{14}, \ldots, E_{18}$ on circle C_3. The numerical locations of all equilibrium points on circles C_1, C_2 and C_3 for various values of mass parameter β are given in Tables 1, 2 and 3, respectively. This is also observed that as the mass parameter β increases, the radius of circle C_1 and C_2 increases while the radius of circle C_3 decreases. Hence the equilibrium points on C_1 and C_2 move away from the peripheral primaries and the equilibrium points on C_3 come closer to central primary (Fig. 8).

4 Stability of equilibrium points in orbital plane

In this section, we study the possible motion of infinitesimal mass around all the equilibrium points $E_1, E_2, \ldots, E_{18}$. Instead of discussing the stability of all equilibrium points we focus only on one equilibrium point on each circle C_1, C_2 and C_3, respectively. The stability of one equilibrium point on any circle C_1, C_2 and C_3 implies the stability of other equilibrium points on the same circle. Therefore, let us assume that the coordinates of these equilibrium points are (x_0, y_0). On giving small displacement (ζ, η) to (x_0, y_0) and considering only linear terms in ζ and η, the variation ζ and η can be written as: $\zeta = x – x_0$ and $\eta = y – y_0$ and the equation of the motion (1) become

$$\left.\begin{aligned} \ddot{\zeta} - 2\,\dot{\eta} &= U_x(x_0+\zeta, y_0+\eta) = \zeta\,\overset{o}{U}_{xx} + \eta\,\overset{o}{U}_{xy}, \\ \ddot{\eta} + 2\,\dot{\zeta} &= U_y(x_0+\zeta, y_0+\eta) = \zeta\,\overset{o}{U}_{yx} + \eta\,\overset{o}{U}_{yy}\,. \end{aligned}\right\} \tag{7}$$

The characteristic equation of Eq. (7) is given by

$$\Pi^4 + (4 - \underset{xx}{\overset{o}{U}} - \underset{yy}{\overset{o}{U}})\,\Pi^2 + \underset{xx}{\overset{o}{U}}\,\underset{yy}{\overset{o}{U}} - (\underset{xy}{\overset{o}{U}})^2 = 0 \tag{8}$$

is a fourth degree equation in Π, where

$$\underset{xx}{\overset{o}{U}} = \left.\frac{\partial^2 U}{\partial x^2}\right|_{(x_0, y_0)} = 1 - \frac{1}{r_{00}^3}\left(1 - \frac{3x_o^2}{r_{00}^2}\right) - \beta\sum_{\upsilon=1}^{6}\frac{1}{r_{0\upsilon}^3}\left(1 - \frac{3(x_0 - x_\upsilon)^2}{r_{0\upsilon}^2}\right),$$

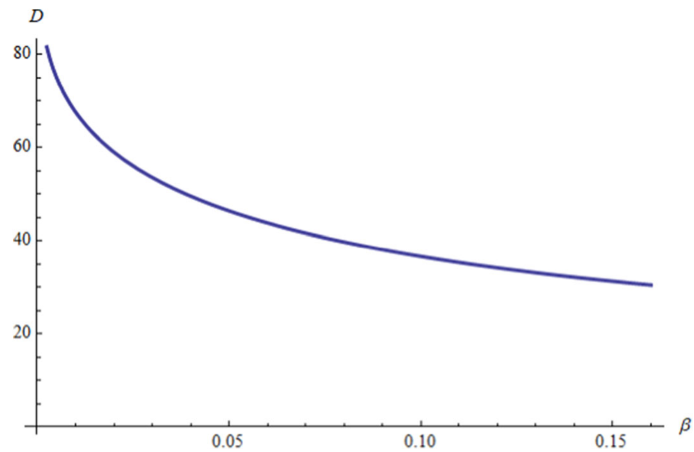

Fig. 9 D with respect to β for E_1

$$\overset{o}{U}_{xy} = \frac{\partial}{\partial x}\left(\frac{\partial U}{\partial y}\right)\Big|_{(x_0,y_0)} = \frac{\partial}{\partial y}\left(\frac{\partial U}{\partial x}\right)\Big|_{(x_0,y_0)} = \overset{o}{U}_{yx} = \frac{3x_o y_o}{r_{00}^5} + 3\beta\sum_{\upsilon=1}^{6}\frac{(x_o - x_\upsilon)(y_o - y_\upsilon)}{r_{0\upsilon}^5},$$

$$\overset{o}{U}_{yy} = \frac{\partial^2 U}{\partial y^2}\Big|_{(x_0,y_0)} = 1 - \frac{1}{r_{00}^3}\left(1 - \frac{3y_o^2}{r_{00}^2}\right) - \beta\sum_{\upsilon=1}^{6}\frac{1}{r_{0\upsilon}^3}\left(1 - \frac{3(y_0 - y_\upsilon)^2}{r_{0\upsilon}^2}\right),$$

$$r_{00}^2 = x_o^2 + y_o^2, r_{0\upsilon}^2 = (x_o - x_\upsilon)^2 + (y_o - y_\upsilon)^2,\ \upsilon = 1,\ 2,\ ...,\ 6.$$

Let $\Pi^2 = \chi$, therefore the characteristic Eq. (8) becomes

$$\chi^2 + (4 - \overset{o}{U}_{xx} - \overset{o}{U}_{yy})\,\chi + \overset{o}{U}_{xx}\,\overset{o}{U}_{yy} - (\overset{o}{U}_{xy})^2 = 0 \tag{9}$$

which is a quadratic equation in χ. If χ_1 and χ_2 are the roots of Eq. (9) then

$$\chi_{1,2} = \frac{1}{2}\left(-p \pm \sqrt{D}\right), \tag{10}$$

where D is the discriminant of Eq. (9) and defined as $D = p^2 - 4q$, $p = 4 - \overset{o}{U}_{xx} - \overset{o}{U}_{yy}$, $q = \overset{o}{U}_{xx}\,\overset{o}{U}_{yy} - (\overset{o}{U}_{xy})^2$.

Therefore, the roots corresponding to characteristic Eq. (8) are given by

$$\Pi_{1,2} = \pm\sqrt{\chi_1} \text{ and } \Pi_{3,4} = \pm\sqrt{\chi_2}. \tag{11}$$

The equilibrium point (x_0, y_0) is said to be stable if $\chi_{1,2} < 0$.

4.1 Stability of equilibrium points on $\boldsymbol{C}_1$

For E_1: The discriminant of Eq. (9) is positive, i.e., $D > 0$ for all values of mass parameter β (Fig. 9) and thus the roots of Eq. (9) are real and unequal. The roots of Eq. (9), i.e., $\chi_{1,2}$ for different values of mass parameter μ are plotted in Fig. 10 and it is observed that $\chi_1 > 0$ and $\chi_2 < 0$ and hence the roots of characteristic Eq. (8) are of the form $\Pi_{1,2} = \pm u$ and $\Pi_{3,4} = \pm iv$, u, $v \in \boldsymbol{R}$ which leads to instability of equilibrium point E_1 (Table 4). Hence the other equilibrium points on C_1 are also unstable for all values of mass parameter μ.

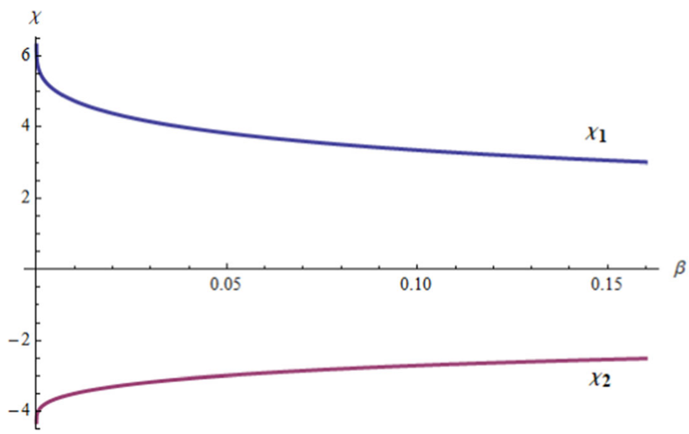

Fig. 10 $\chi_{1,2}$ with respect to β for E_1

Table 4 Stability of E_1

B	χ_1	χ_2	$\Pi_{1,2}$	$\Pi_{3,4}$	Stability
0.01	4.73307	− 3.48829	±2.17556	±1.86771i	Unstable
0.02	4.38325	− 3.29769	±2.09362	±1.81596i	Unstable
0.04	3.97134	− 3.06726	±1.99282	±1.75136i	Unstable
0.06	3.70371	− 2.91425	±1.92450	±1.70712i	Unstable
0.08	3.50452	− 2.79885	±1.87204	±1.67298i	Unstable
0.10	3.34651	− 2.70646	±1.82935	±1.64513i	Unstable
0.12	3.21629	− 2.62981	±1.79340	±1.62167i	Unstable
0.14	3.10620	− 2.56467	±1.76244	±1.60146i	Unstable
0.16	3.01137	− 2.50833	±1.73533	±1.58377i	Unstable

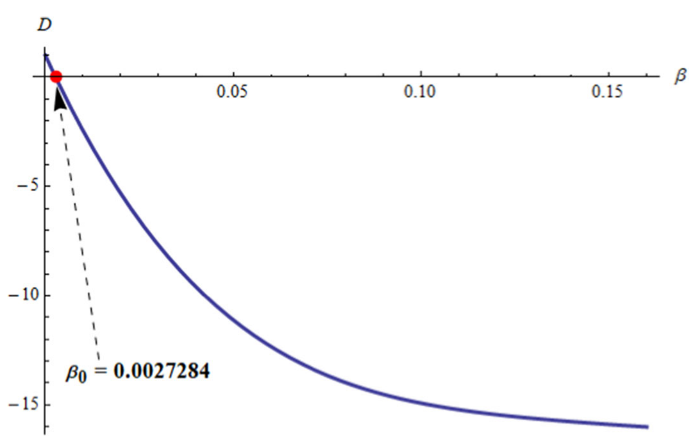

Fig. 11 D with respect to β for E_8

4.2 Stability of equilibrium points on $\boldsymbol{C}_2$

For E_8: $D \geq 0$ if and only if $0 < \beta \leq 0.0027284$ (Fig. 11) and thus Eq. (9) possesses real roots in the interval $0 < \beta \leq 0.0027284$. The roots of Eq. (9), i.e., $\chi_{1,2}$ for $0 < \beta \leq 0.0027284$ are plotted in Fig. 12 and it is observed that $\chi_1 < 0$ and $\chi_2 < 0$ and hence the roots of characteristic Eq. (8) are of the form $\Pi_{1,2} = \pm iu_1$ and $\Pi_{3,4} = \pm iv_1$, $u_1, v_1 \in \boldsymbol{R}$ which leads to stability of equilibrium point E_8 (Table 5). Hence the other equilibrium points on C_2 are also stable for the critical mass parameter $0 < \beta \leq \beta_0$, $\beta_0 = 0.0027284$.

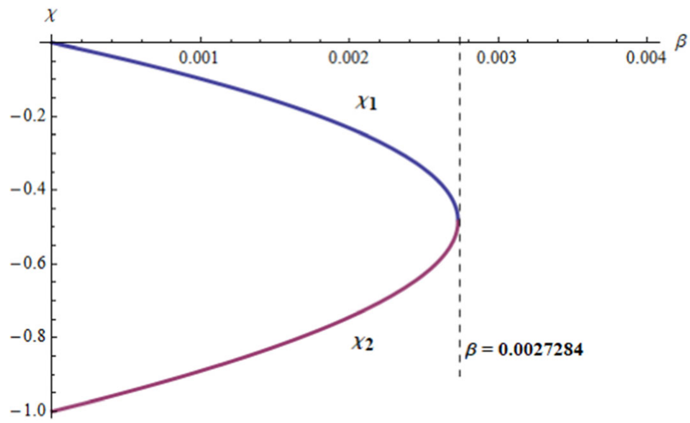

Fig. 12 $\chi_{1,2}$ with respect to β for E_8

Table 5 Stability of E_8

B	χ_1	χ_2	$\Pi_{1,2}$	$\Pi_{3,4}$	Stability
0.0001	− 0.00885	− 0.98992	±0.09408i	±0.99495i	Stable
0.0010	− 0.09767	− 0.89012	±0.31252i	±0.94346i	Stable
0.0020	− 0.23173	− 0.74392	±0.48138i	±0.86251i	Stable
0.0025	− 0.34171	− 0.62789	±0.58456i	±0.79239i	Stable
0.0026	− 0.37696	− 0.59144	±0.61397i	±0.77691i	Stable
0.00269	− 0.42503	− 0.54228	±0.65194i	±0.73639i	Stable
0.00270	− 0.43318	− 0.53401	±0.65817i	±0.73076i	Stable
0.00272	− 0.45606	− 0.51089	±0.67532i	±0.71477i	Stable
0.002725	− 0.46599	− 0.50089	±0.68264i	±0.70774i	Stable
0.002728	− 0.47743	− 0.48943	±0.69096i	±0.69959i	Stable
0.0027282	− 0.47917	− 0.48769	±0.69222i	±0.69834i	Stable
0.0027284	− 0.48293	− 0.48392	±0.69493i	±0.69564i	Stable
0.0027285	− 0.48343 + 0.00295i	− 0.48343 − 0.00295i	±0.00212 + 0.69529i	±0.00212 − 0.69529i	Unstable
0.003	− 0.48179 + 0.15569i	− 0.48179 − 0.15569i	±0.11075 + 0.70289i	±0.11075 − 0.70289i	Unstable
0.005	− 0.46983 + 0.44635i	− 0.46983 − 0.44635i	±0.29851 + 0.74762i	±0.29851 − 0.74762i	Unstable
0.01	− 0.44055 + 0.78123i	− 0.44055 − 0.78123i	±0.47767 + 0.81775i	±0.47767 − 0.81775i	Unstable
0.05	− 0.23813 + 1.66769i	− 0.23813 − 1.66769i	±0.85043 + 0.98046i	±0.85043 − 0.98046i	unstable
0.10	− 0.06409 + 1.93181i	− 0.06409 − 1.93181i	±0.96664 + 0.99924i	±0.96664 − 0.99924i	unstable
0.12	− 0.01816 + 1.96534i	− 0.01816 − 1.96534i	±0.98672 + 0.99588i	±0.98672 − 0.99588i	unstable
0.14	0.015809 + 1.98567i	0.015809 − 1.98567i	±1.00039 + 0.99245i	±1.00039 − 0.99245i	unstable
0.16	0.039618 + 2.00089i	0.039618 − 2.00089i	±1.01017 + 0.99037i	±1.01017 − 0.99037i	unstable

4.3 Stability of equilibrium points on $\boldsymbol{C}_3$

For E_{13}: $D > 0$ for all values of mass parameter β (Fig. 13) and thus the roots of Eq. (9) are real and unequal. The roots of Eq. (9), i.e., $\chi_{1,2}$ for different values of mass parameter β are plotted in Fig. 14 and it is observed that $\chi_1 > 0$ and $\chi_2 < 0$ and hence the roots of characteristic Eq. (8) are of the form $\Pi_{1,2} = \pm u_2$ and $\Pi_{3,4} = \pm iv_2$, $u_2, v_2 \in \boldsymbol{R}$ which leads to instability of equilibrium point E_{13} (Table 6). Hence the other equilibrium points on C_2 are also unstable for all values of mass parameter β.

5 Regions of motion

In this section, the regions of motion for a fixed value of mass parameter β and different values of Jacobi constant c have been plotted. The values of Jacobi constant c are computed numerically at all the equilibrium points ($E_1, E_2, \ldots, E_{18}$) using Eq. $2U–c = 0$ in Table 7. Figure 15a, the zero velocity regions have been plotted for $c = 3.5$ and a circular white region around the central primary has been observed. The white and shaded regions correspond to permitted and restricted regions of motion, respectively for the motion of infinitesimal mass. For $c = 3.25$, some small white regions appear around the primaries P_1, P_2, P_3, P_5 and P_6 which allow to move infinitesimal mass in the vicinity of P_1, P_2, P_3, P_5 and P_6 only (Fig. 15b). For $c = c_3$, a transition

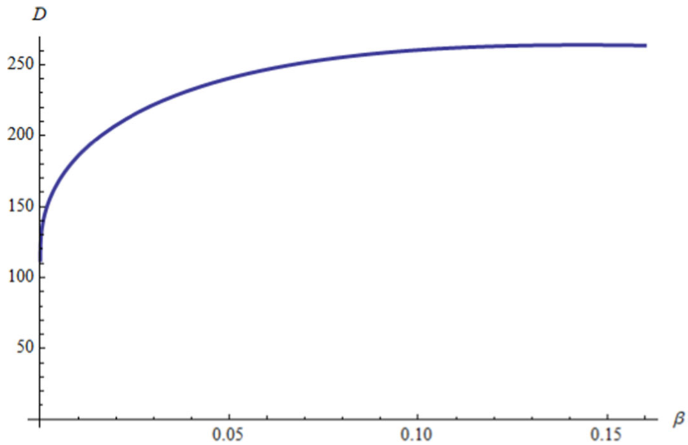

Fig. 13 D with respect to β for E_{13}

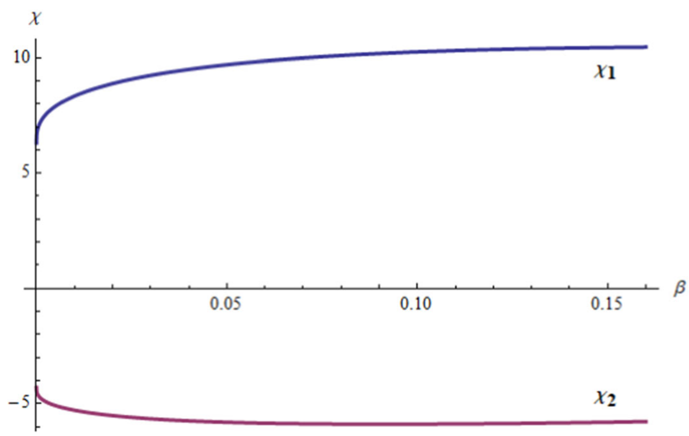

Fig. 14 $\chi_{1,2}$ with respect to β for E_{13}

Table 6 Stability of E_{13}

B	χ_1	χ_2	$\Pi_{1,2}$	$\Pi_{3,4}$	Stability
0.01	8.34174	− 5.28553	± 2.88882	± 2.29903i	Unstable
0.02	8.88364	− 5.51826	± 2.98054	± 2.34910i	Unstable
0.04	9.49928	− 5.74653	± 3.08209	± 2.39719i	Unstable
0.06	9.86006	− 5.84715	± 3.14007	± 2.41809i	Unstable
0.08	10.0935	− 5.88563	± 3.17702	± 2.42603i	Unstable
0.10	10.2489	− 5.88740	± 3.20139	± 2.42641i	Unstable
0.12	10.3517	− 5.86546	± 3.21741	± 2.42187i	Unstable
0.14	10.4170	− 5.82747	± 3.22754	± 2.41402i	Unstable
0.16	10.4547	− 5.77835	± 3.23337	± 2.40382i	Unstable

exists at the equilibrium points E_{13}, E_{14}, E_{15}, E_{16}, E_{17} and E_{18} which allow the infinitesimal mass to move from central primary to other peripheral primaries but it cannot move to the outer region, Fig. 15c. For $c = c_1$, again some transitions exist at the equilibrium points E_1, E_2, E_3 E_4, E_5 and E_6 which allow the infinitesimal mass to move from E_{13}, E_{14}, E_{15}, E_{16}, E_{17} and E_{18} to outer region and the forbidden region constitutes six branches containing equilibrium points E_7, E_8, E_9, E_{10}, $E_{11}$and E_{12}, respectively, Fig. 15d. For $c = 3.015$, the forbidden region get reduced and the infinitesimal mass is allowed to move in the entire xy-plane except the forbidden region containing equilibrium points E_7, E_8, E_9, E_{10}, E_{11} and E_{12}, Fig. 15e. For $c = c_2$, all the forbidden regions has been disappeared and the infinitesimal mass can move in the entire xy-plane, Fig. 15f. Thus, it is observed that the forbidden region decreases as the value of Jacobi constant c decreases.

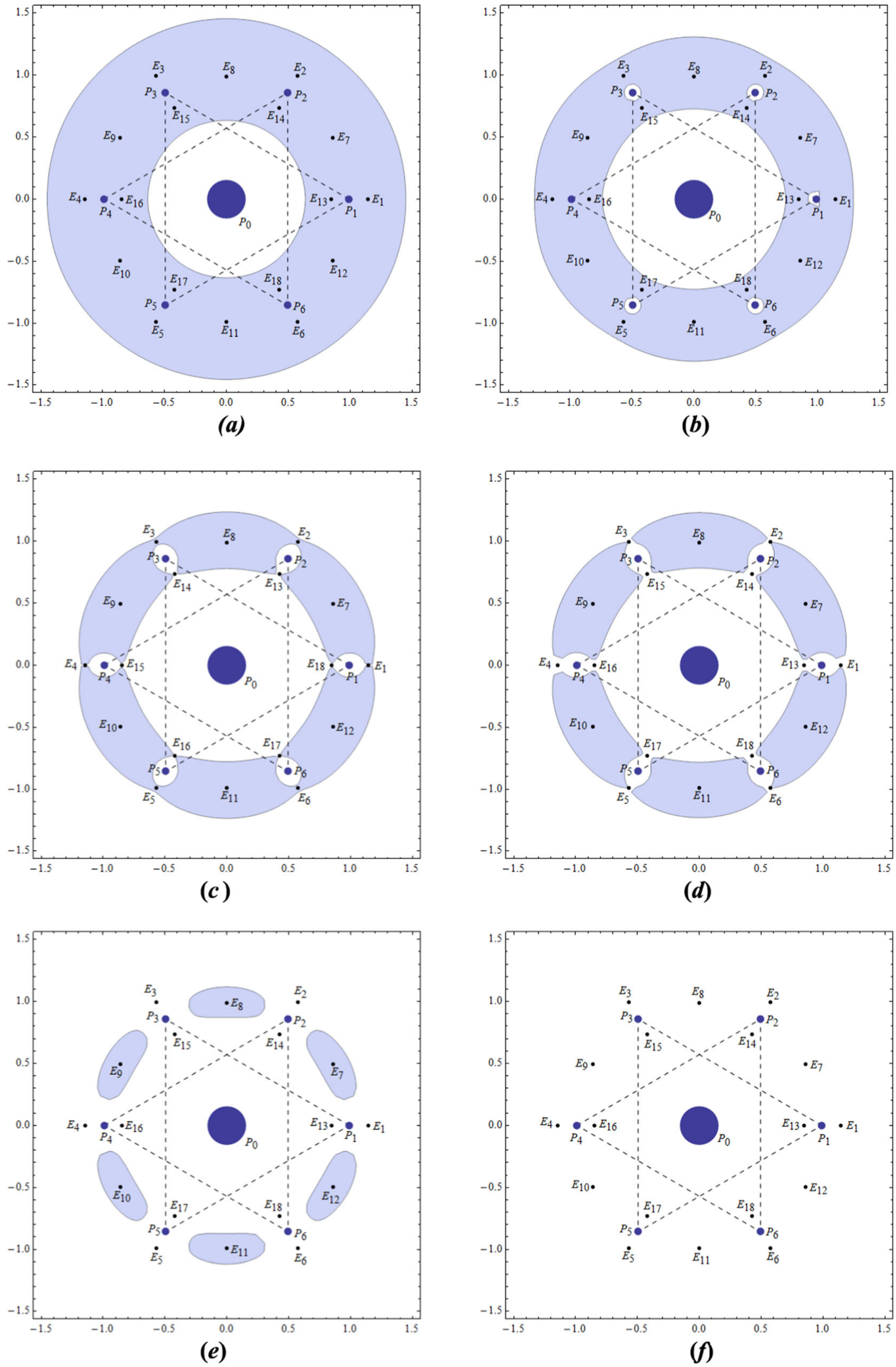

Fig. 15 Regions of motion for $\beta = 0.01$ and different values of Jacobi constant c; ***a***: $c = 3.5$; ***b***: $c = 3.4$; ***c***: $c = 3.28$; ***d***: $c = 3.265$; ***e***: $c = c_1$; ***f***: $c = c_2$

Table 7 Jacobi constant c at E_i ($i = 1, 2, \ldots, 18$) for $\beta = 0.01$

Equilibrium points	x_0	y_0	*Jacobi constant c*
E_1	1.162940	0	$c_1 = 3.1636$
E_2	0.581470	1.007136	
E_3	− 0.581470	1.007136	
E_4	− 1.162940	0	
E_5	− 0.581470	− 1.007136	
E_6	0.581470	− 1.007136	
E_7	0.875263	0.505333	$c_2 = 3.00682$
E_8	0	1.010666	
E_9	− 0.875263	0.505333	
E_{10}	− 0.875263	− 0.505333	
E_{11}	0	− 1.010666	
E_{12}	0.875263	− 0.505333	
E_{13}	0.863812	0	$c_3 = 3.14097$
E_{14}	0.431906	0.748083	
E_{15}	− 0.431906	0.748083	
E_{16}	− 0.863812	0	
E_{17}	− 0.431906	− 0.748083	
E_{18}	0.431906	− 0.748083	

6 Conclusion

We have studied the dynamics of infinitesimal mass around the equilibrium points in the restricted eight-body problem. This problem is a particular case of n + 1-body problem studied by Kalvouridis [27]. In this paper, we considered six peripheral primaries P_1, P_2, …, P_6, each of mass m, revolve in a circular orbit of radius a with an angular velocity ω about their common center of mass O. The primaries P_i ($i = 1, 2, \ldots, 6$) are revolve in a way such that P_1, P_3, P_5 and P_2, P_4, P_6 always form equilateral triangles of side l and have a common circumcenter where the seventh more massive primary P_0 of mass m_0 rests. The equations of motion for the infinitesimal mass in synodic coordinate system and dimensionless variables are given by Eq. (1). On solving the Eqns. $U_x(x, y) = 0, U_y(x, y) = 0$ and $z = 0$ we found 18 equilibrium points such that four equilibrium points are on x-axis, two on y-axis and rest are in orbital plane of the primaries. All the equilibrium points lie on the concentric circles C_1, C_2 andC_3 centered at origin. It is observed that as the mass parameter β increases, the radius of circles C_1 and C_2 also increases and the equilibrium points on C_1 and C_2 move away from the peripheral primaries. On the other hand, the radius of circle C_3 decreases as β increases and the equilibrium points on C_3 come closer to the central primary. The stability of equilibrium points depends upon the nature of roots of characteristic Eq. (8). On solving the characteristic Eq. (8) for various values of mass parameter β in the interval $0 < \beta < 1/6$ we found that the equilibrium points on circle C_2 are stable for the critical mass parameter β_0 while the equilibrium points on circles C_1 and C_3 are unstable for all values of mass parameter β. In the last section of this paper, the regions of motion for infinitesimal mass are investigated and it is found that the forbidden region decreases as the value of Jacobi constant c decreases.

Declarations

Conflict of interest The authors declare that there is no conflict of interests regarding publication of this manuscript.

References

1. Ansari, A.A.: The circular restricted four-body problem with triaxial primaries and variable mass. Appl. Appl. Math. **13**, 818–838 (2018)
2. Baltagiannis, A.N., Papadakis, K.E.: Equilibrium points and their stability in the restricted four-body problem. Int. J. Bifurc. Chaos **21**(8), 2179–2193 (2011)
3. Bang, D., Elmabsout, B.: Restricted N+1-body problem: existence and stability of relative equilibria. Celest. Mech. Dyn. Astron. **89**, 305–318 (2004)
4. Bhatnagar, K.B., Hallan, P.P.: Effect of perturbed potentials on the stability of libration points in the restricted problem. Celest. Mech. **20**, 95–103 (1979)

5. Casasayas, J., Nunes, A.: A restricted charged four-body problem. Celest. Mech. Dyn. Astron. **47**, 245–266 (1990)
6. Celli, M.: The central configurations of four masses *x, -x, y, -y*. J. Differ. Eq. **235**, 668–682 (2007)
7. Chen, J., Yang, M.: Central configurations of the 5-body problem with four infinitesimal particles. Few-Body Syst. **61**, 26 (2020)
8. Chernikov, Y.A.: The photogravitational restricted three body problem. Soviet Astronomy-AJ **14**, 176–181 (1970)
9. Choudhary, R.K.: Libration points in the generalized elliptic restricted three body problem. Celest. Mech. **16**, 411–419 (1977)
10. Cid, R., Ferrer, S., Caballero, J.A.: Asymptotic solutions of the restricted problem near equilateral Lagrangian points. Celest. Mech. Dyn. Astron. **35**, 189–200 (1985)
11. Corbera, M., Cors, J.M., Llibre, J.: On the central configurations of the planar 1+3 body problem. Celest. Mech. Dyn. Astron. **109**, 27–43 (2011)
12. Danby, J.M.A.: Stability of the triangular points in the elliptic restricted problem of three bodies. Astron. J. **69**(2), 165–172 (1964)
13. Davis, C., Geyer, S., Johnson, W., Xie, Z.: Inverse problem of central configurations in the collinear 5-body problem. J. Math. Phys. **59**, 052902 (2018)
14. Douskos, C.N.: Collinear equilibrium points of Hill's problem with radiation and oblateness and their fractal basins of attraction. Astrophys. Space Sci. **326**, 263–271 (2010)
15. Ershkov, S.V., Leshchenko, D.: Solving procedure for 3D motions near libration points in CR3BP. Astrophys. Space Sci. **364**, 207 (2019)
16. Ershkov, S., Leshchenko, D., Prosviryakov, Y.: Semi-analytical approach in BiER4BP for exploring the stable positioning of the elements of a Dyson sphere. Symmetry **15**, 326 (2023)
17. Gao, C., Yuan, J., Sun, C.: Equilibrium points and zero velocity surfaces in the axisymmetric five-body problem. Astrophys. Space Sci. **362**, 72 (2017)
18. Idrisi, M.J., Taqvi, Z.A.: Restricted three-body problem when one of the primaries is an ellipsoid. Astrophys. Space Sci. **348**, 41–56 (2013)
19. Idrisi, M.J.: Existence and stability of the non-collinear libration points in the restricted three body problem when both the primaries are ellipsoid. Astrophys. Space Sci. **350**, 133–141 (2014)
20. Idrisi, M.J.: A study of libration points in modified CR3BP under albedo effect when smaller primary is an ellipsoid. J. Astronaut. Sci. **64**, 379–398 (2017)
21. Idrisi, M.J., Ullah, M.S.: Non-collinear libration points in ER3BP with albedo effect and oblateness. J. Astrophys. Astron. **39**, 28 (2018)
22. Idrisi, M.J., Ullah, M.S.: A study of albedo effects on libration points in the elliptic restricted three-body problem. J. Astronaut. Sci. **67**, 863–879 (2020a)
23. Idrisi, M.J., Ullah, M.S.: Central-body square configuration of restricted-six body problem. New Astron. **79**, 101381 (2020b)
24. Idrisi, M.J., Ullah, M.S., Sikkandhar, A.: Effect of perturbations in coriolis and centrifugal forces on equilibrium points in the restricted six-body problem. J. Astronaut. Sci. **68**, 4–25 (2021)
25. Idrisi, M.J., Ullah, M.S.: Out-of-plane equilibrium points in the elliptic restricted three-body problem under albedo effect. New Astron. **89**, 101629 (2021)
26. Idrisi, M.J., Ullah, M.S.: Motion around out-of-plane equilibrium points in the frame of restricted six-body problem under radiation pressure. Few-Body Syst. **63**, 50 (2022)
27. Kalvouridis, T.J.: A planar case of the $n + 1$ body problem: the 'Ring' problem. Astrophys. Space Sci. **260**, 309–325 (1999)
28. Kumari, R., Kushvah, B.S.: Equilibrium points and zero velocity surfaces in the restricted four-body problem with solar wind drag. Astrophys. Space Sci. **344**, 347–359 (2013)
29. Kumari, R., Pal, A.K., Bairwa, L.K.: Periodic solution of circular Sitnikov restricted four-body problem using multiple scales method. Arch. Appl. Mech. **92**, 3847–3860 (2022)
30. Marchesin, M.: Stability of a rhomboidal configuration with a central body. Astrophys. Space Sci. **362**, 1–13 (2017)
31. Markellos, V.V., Papadakis, K.E., Perdios, E.A.: Non-linear stability zones around triangular equilibria in the plane circular restricted three-body problem with oblateness. Astrophys. Space Sci. **245**, 157–164 (1996)
32. Michalodimitrakis, M.: The circular restricted four-body problem. Astrophys. Space Sci. **75**, 289–305 (1981)
33. Pacella, F.: Central configurations of the N-body problem via equivariant Morse theory. Arch. Rat. Mech. Anal. **97**, 59–74 (1987)
34. Papadouris, J.P., Papadakis, K.E.: Equilibrium points in the photogravitational restricted four-body problem. Astrophys. Space Sci. **344**, 21–38 (2013)
35. Pappalarado, C.M., Lettieri, A., Guida, D.: Stability analysis of rigid multibody mechanical systems with holonomic and nonholonomic constraints. Arch. Appl. Mech. **90**, 1961–2005 (2020)
36. Qiu-Dong, W.: The global solution of the *N*-body problem. Celest. Mech. Dyn. Astron. **50**, 73–88 (1990)
37. Roberts, G.E.: Linear stability of the elliptic lagrangian triangle solutions in the three-body problem. J. Differ. Eq. **182**(1), 191–218 (2002)
38. Roy, A.E., Steves, B.A.: Some special restricted four-body problems–II. From caledonia to copenhagen. Planetary Space Sci. **46**, 1475–1486 (1998)
39. Siddique, M.A.R., Kashif, A.R., Shoaib, M., Hussain, S.: Stability analysis of the rhomboidal restricted six-body problem. Adv. Astronomy **6**, 1–15 (2021)
40. Siddique, M.A.R., Kashif, A.R.: The restricted six-body problem with stable equilibrium points and a rhomboidal configuration. Adv. Astronomy **2022**, 8100523 (2022)
41. Szebehely, V.: Theory of orbits. The restricted problem of three bodies. Academic Press, New York and London (1967)
42. Turyshev, S.G., Toth, V.T.: New perturbative method for solving the gravitational N-body problem in the general theory of relativity. Int. J. Modern Phys. **24**, 1550039 (2015)
43. Ullah, M.S., Idrisi, M.J., Kumar, V.: Elliptic Sitnikov five-body problem under radiation pressure. New Astron. **80**, 101398 (2020)

44. Ullah, M.S., Idrisi, M.J., Sharma, B.K., Kaur, C.: Sitnikov five-body problem with combined effects of radiation pressure and oblateness. New Astron. **87**, 101574 (2021)